

Short-time behavior in multiphoton ionization

Constantine E. Theodosiou* and Lloyd Armstrong, Jr.†

Department of Physics, The Johns Hopkins University, Baltimore, Maryland 21218

M. Crance and S. Feneuille

Laboratoire Aimé Cotton, Centre National de la Recherche Scientifique II, Bâtiment 505, 91405-Orsay, France

(Received 16 March 1978)

The short-time behavior of atomic multiphoton-ionization profiles is investigated using simplified models of the field and the atom. The importance of including many levels in the model atom, of spontaneous emission, and of pulse shape are studied in detail. It is shown that the first two of these have little influence on the qualitative behavior of the short-time behavior of the resonance profile, but that the third, the pulse shape, is critical in determining the time evolution of the resonance profile.

I. INTRODUCTION

In a recent article, Beers and Armstrong¹ (to be referred to as BA) introduced a simplified model of resonant two-photon ionization which could be solved exactly. One of the more interesting results obtained from this model had to do with the time development of resonance profiles, that is, dependence of the profile on the pulse length of the ionizing radiation. It was found that under certain conditions, the prominent aspects of the ionization profile—the pronounced maximum and the interference minimum—will not be observed.

However, there are a large number of effects which are not included in this relatively simple model of BA which might well affect its predictions. In this paper, we investigate more accurate models of multiphoton ionization incorporating three improvements to the BA model which seemed most likely to change the time evolution of the resonant profile as predicted by BA. Specifically (a) we treat explicitly an atom with more than one intermediate state; (b) we examine the effects of spontaneous emission from the intermediate resonant state; (c) we study the effects of laser-light pulse shape.

Since the predictions of the BA model usually qualitatively meet and will be used as a reference point in our study and discussion, we briefly review that model's main features and its predictions concerning the time development of the resonance profile.

The model of BA explicitly involved only two bound states of the atom—a ground state $|g\rangle$ and a “resonant” excited state $|a\rangle$. The effects of the other “nonresonant” bound states of the atom were introduced through an effective two-photon term H_{eff} in the atom-field Hamiltonian. The field itself was assumed to be initially composed of n photons

of energy ω ($\hbar=1$). The atom-field interaction was abruptly turned on at $t=0$ and off at $t=T$; this corresponds classically to a rectangular pulse of radiation of length T . The solutions to this model were found to be characterized by five parameters: the detuning from resonance

$$\delta = (E_g + n\omega) - [E_a + (n-1)\omega] = E_g + \omega - E_a; \quad (1)$$

the matrix element of the atom-field interaction H_{AF} between ground and intermediate states

$$H_{ga} = (g, n\omega | H_{AF} | a, (n-1)\omega), \quad (2)$$

where $|g, n\omega\rangle$ is an atom-field state in which the atom is in the state $|g\rangle$, and n photons of energy ω are present, etc.; the rate of the ionization of the intermediate state

$$\gamma_a = 2\pi |(a, (n-1)\omega | H_{AF} | E, (n-2)\omega)|^2 = 2\pi H_{aE}^2, \quad (3)$$

where $|E\rangle$ is a state of the ionized atom plus a photoelectron having total energy E ; the rate of two-photon ionization of the ground state through all intermediate levels other than $|a\rangle$

$$\gamma_g = 2\pi |(g, n\omega | H_{\text{eff}} | E, (n-2)\omega)|^2 = 2\pi |H_{gE}|^2; \quad (4)$$

and

$$q = H_{ga} / \pi H_{gE} H_{Ea}. \quad (5)$$

Using this model, it was found that for short pulses the predicted resonance profile was quite flat, with no sharp maximum at the resonance position, and no deep minimum produced by interference between the ionization path $|g\rangle \rightarrow |a\rangle \rightarrow |E\rangle$ and all other paths whose effects were described by H_{eff} . For longer pulses, the maximum began to grow, and the interference minimum began to deepen. The development of maximum and minimum did not, however, generally proceed on the same time scale. Both maximum and minimum were seen to shift their position as they developed,

with the minimum undergoing a quite substantial displacement in the direction of the "resonant" state $|a\rangle$.

The "characteristic time" for development of the maximum was found to be $\tau_{\max}=1/|H_{ga}|$; and for the development of the minimum, to be $\tau_{\min}=1/\gamma_a$. In most cases, it was found that ionization rates could be defined in the region of the profile near the minimum, but that one rate

$$\sigma_1 = \frac{1}{2}\gamma_g [1 + (q\gamma_a + \delta)^2 / (\delta^2 + 4|H_{ga}|^2)] \quad (6)$$

having only a very broad and shallow minimum held for $T \ll \tau_{\min}$, and another rate

$$\sigma_2 = \gamma_g [(2\delta + q\gamma_a)^2 / (4\delta^2 + \gamma_a^2)] \quad (7)$$

having a sharp and deep minimum held for $T \gg \tau_{\min}$. If H_{gE} is evaluated using the lowest nonvanishing order of perturbation theory, the cross section σ_2 is identical to that obtained using perturbation theory. σ_2 had also previously been obtained by Armstrong *et al.*² using an analogy with autoionization which was valid for $\gamma_a \gg |H_{ga}|, \gamma_g$. The rate σ_1 had previously been obtained by Feneuille and Armstrong³ for the case $|H_{ga}| \gg \gamma_a, \gamma_g$ using a type of perturbation approach. If $\gamma_a \gg |H_{ga}| \gg \gamma_g$, or $|H_{ga}| \gg \gamma_a \gg \gamma_g$, then the region of the maximum could be described by an ionization rate for times $T \gg \tau_{\max}$.

In the following sections, we shall introduce the more accurate models of photoionization, and investigate the effects on the time evolution of the resonance profile brought about by the new effects incorporated into the models. In Sec. II, we consider a model atom having several bound states instead of only two; in Sec. III, the effects of spontaneous emission from the intermediate resonant state are investigated; and in Sec. IV, we study the effect of pulse shape on the time evolution. We shall discuss our results in Sec. V, and show that they can easily be understood in terms of a competition between the "two-step" and "two-photon" modes of ionization. In Sec. VI, we state our conclusions, and the Appendix outlines an efficient approach to numerically evaluating the time evolution of the resonance profile.

II. MANY-LEVEL ATOM

In order to ascertain whether or not the results of BA were produced by incorrect handling of the "nonresonant" states, i.e., by introducing them only through an effective two-photon Hamiltonian H_{eff} , we have introduced a model in which several of the nonresonant levels are treated on an equal mathematical footing with the resonant level. The situation is as indicated in Fig. 1: the model now contains several intermediate states which can be reached from the ground state by absorption of one

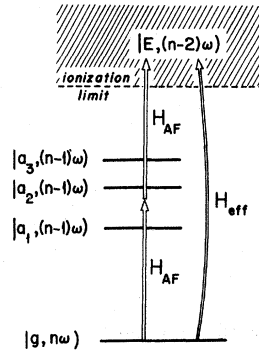


FIG. 1. Two-photon ionization involving several intermediate levels $|a_i, (n-1)\omega\rangle$. The effects of all other levels in the atom are introduced through the effective operator H_{eff} .

photon, with ionization being produced by absorption of a second photon. The effects of all other levels in the atom are still introduced through a new two-photon operator H_{eff} . We will discuss results obtained using three intermediate states $|a_i, (n-1)\omega\rangle$, $i=1-3$. However, calculations have also been made using four and five intermediate states, with no significant changes being observed in the results.

Although for present purposes it is not absolutely necessary to discuss the exact form of H_{eff} , it is convenient to do so in order to indicate how the many-level model could be applied to calculations involving real atoms, especially since the relevant question usually arises when referring to the BA model.

The complete Green's function equation for this problem can be written quite generally as

$$(z - H_0 - H_{\text{AF}})G = 1, \quad (8)$$

where H_0 is the sum of the atomic and field Hamiltonians. Let us define the projector operators:

$$Q = 1 - |g, n\omega\rangle\langle g, n\omega| - \sum_{i=1}^3 |a_i, (n-1)\omega\rangle\langle a_i, (n-1)\omega| - \int dE |E, (n-2)\omega\rangle\langle E, (n-2)\omega| \quad (9)$$

and

$$P = 1 - Q. \quad (10)$$

We wish to consider the Green's function equations on the space left invariant by P .⁴ In order to find these equations, consider

$$P(z - H_0 - H_{\text{AF}})(P + Q)G|g, n\omega\rangle = |g, n\omega\rangle \quad (11)$$

and

$$Q(z - H_0 - H_{\text{AF}})(P + Q)G|g, n\omega\rangle = 0 \quad (12)$$

which follow directly from (8)–(10). Solving the second equation for QG one finds

$$QG|g, n\omega\rangle = Q \frac{1}{z - H_0 - QH_{\text{AF}}Q} QH_{\text{AF}}PG|g, n\omega\rangle. \quad (13)$$

Inserting this in the first equation gives

$$P(z-H_0-H_{AF}-H_{AF}KH_{AF})PG|g,n\rangle=|g,n\rangle, \quad (14)$$

where

$$K=Q\frac{1}{z-H_0-QH_{AF}Q}. \quad (15)$$

The effects of all the states of the atom not contained in the space which is invariant under P are then contained in the term $H_{AF}KH_{AF}$; we identify this as

$$H_{\text{eff}}(z)\equiv H_{AF}KH_{AF}. \quad (16)$$

If the states left invariant by Q are truly nonresonant, then $H_{\text{eff}}(z)$ will have only a slight dependence on z in the regions of the poles of PG . Thus one can approximate $H_{\text{eff}}(z)$ by its value near to one of the poles, e.g., at $z\approx E_g+n\omega$. We can then define this as the effective Hamiltonian for our problem

$$H_{\text{eff}}\cong H_{\text{eff}}(z\cong E_g+n\omega)=H_{AF}K(z=E_g+n\omega)H_{AF}.$$

To make the many-level model completely mathematically correct, one should further replace H_{AF} by

$$H_{AF}+H_{\text{eff}}$$

in the matrix elements used below, Eqs. (20). We shall not bother to do this, however, since in the model problem we are considering these matrix elements are simply parameters to be varied and their explicit forms are unimportant.

Consider now the time-dependent Schrödinger equation for this system.

$$(H_0+H_{AF}+H_{\text{eff}})\psi(t)=H\psi(t)=i\frac{\partial}{\partial t}\psi(t), \quad (17)$$

where

$$\begin{aligned} \psi(t)=\alpha_g(t)|g,n\rangle+\sum_{i=1}^3\alpha_i(t)|a_i,(n-1)\omega\rangle \\ +\int dE\alpha_E(t)|E,(n-2)\omega\rangle. \end{aligned} \quad (18)$$

Inserting (18) into (17), one obtains the equations⁵

$$i\dot{\alpha}_n(t)-W_n\alpha_n(t)=\sum_{m\neq n}H_{nm}\alpha_m(t)+i\delta(t)\delta(n,g), \quad (19)$$

where $n, m=g, \{i\}, \{E\}$, with $\{i\}$ being the set $i=1, 2, 3$, etc. When $m=\{E\}$ the sum above becomes an integral. The remaining quantities in (19) are defined by

$$\begin{aligned} H_{gi}&=(g,n\omega|H_{AF}|a_i,(n-1)\omega), \\ H_{iE}&=(a_i,(n-1)\omega|H_{AF}|E,(n-2)\omega), \\ H_{gE}&=(g,n\omega|H_{\text{eff}}|E,(n-2)\omega), \end{aligned} \quad (20)$$

$$W_m=E_m+n_m\omega.$$

All other matrix elements of H are equal to zero. The δ functions in (19) reflect that the atom is in the state $|g,n\rangle$ at $t=0$.

The coefficients in (19) are then Fourier transformed using

$$\alpha_n(t)=-\frac{1}{2\pi i}\int_{-\infty}^{+\infty}G_n(z)e^{-i(z+W_g)t}dz \quad (21)$$

leading to the algebraic equations

$$(z-\Delta_g)G_g(z)=\sum_{i=1}^3H_{gi}G_i(z)+\int dEH_{gE}G_E(z)+1, \quad (22a)$$

$$(z-\Delta_i)G_i(z)=H_{ig}G_g(z)+\int dEH_{iE}G_E(z), \quad (22b)$$

$$(z-\Delta_E)G_E(z)=H_{Eg}G_g(z)+\sum_{i=1}^3H_{Ei}G_i(z), \quad (22c)$$

where

$$\Delta_n\equiv W_n-W_g. \quad (23)$$

Inserting (22c) into (22a) and (22b), one obtains

$$\left(z-W_g^*(z)+i\frac{\gamma_g(z)}{2}\right)G_g(z)=\sum_{i=1}^3\left(H_{gi}^*(z)-i\frac{\gamma_{gi}(z)}{2}\right)G_i(z)+1 \quad (24)$$

$$\begin{aligned} \left(z-W_i^*(z)+i\frac{\gamma_i(z)}{2}\right)G_i(z)=\sum_{j=1}^3\left(H_{ij}^*(z)-i\frac{\gamma_{ij}(z)}{2}\right)G_j(z) \\ +\left(H_{iE}^*(z)-i\frac{\gamma_{iE}(z)}{2}\right)G_E(z). \end{aligned}$$

where

$$W_i^*(z)=\Delta_i+\mathcal{O}\int dE\frac{|H_{iE}|^2}{z-\Delta_E}, \quad (25)$$

$$\gamma_i(z)=2\pi|H_{iE}|_{\Delta_E=z}^2, \quad (26)$$

$$H_{im}^*(z)=H_{im}+\mathcal{O}\int dE\frac{H_{iE}H_{Em}}{z-\Delta_E}, \quad (27)$$

$$\gamma_{im}(z)=2\pi H_{iE}H_{Em}|_{\Delta_E=z}, \quad (28)$$

for $l, m=g, 1, 2, 3$. If H_{iE} (all l) is a slowly varying function of E , then all of the parameters defined in Eqs. (25)–(28) can be approximated well by replacing z by a value close to one of the poles of $G(z)$, e.g.,

$$W_i^*(z)\cong W_i^*(z=\Delta_i)=W_i^*(W_l-W_g). \quad (29)$$

It should be noted that the parameters so defined are still functions of photon energy ω . We shall,

for our model calculations, make the further simplifying assumption that the parameters are also ω independent; a calculation involving a real atom should, of course, take into account this ω dependence.⁶

Unlike the case in BA, the system of equations (24) is too complicated to be resolved analytically. They can, however, be easily solved numerically if approximations such as (29) are made. One then inserts the resulting values of G_g and G_i in equations such as given by (21) to obtain the coefficients appearing in (18). The resulting probability of ionization is given by

$$P(t) = 1 - |\alpha_g(t)|^2 - \sum_{i=1}^3 |\alpha_i(t)|^2. \quad (30)$$

Alternatively, one can back-transform Eqs. (24), according to (21), to obtain

$$i\dot{\alpha}_l(t) - \left(W_l + W_g - i\frac{\gamma_l}{2} \right) \alpha_l(t) \\ = \sum_{m=1}^3 \left(H_{lm}^* - i\frac{\gamma_{lm}}{2} \right) \alpha_m + i\delta(t)\delta(l, g) \quad (31)$$

for $l, m = g, 1, 2, 3$. These equations can then be numerically integrated in time. This latter approach was found, however, to be considerably less efficient than the algebraic solution of the Fourier-transformed equations for large detunings (see the Appendix).

A typical result obtained by the former approach is shown in Fig. 2. The values in arbitrary units of the parameters used were $H_{gi}^* = H_{gi} = 1$, $\gamma_{gi} = 0.01$, $\gamma_i = \gamma_{ij} = 0.1$, $H_{ij}^* = 0$, and $\gamma_g = 0.001$. The levels g , a_1 , a_2 , and a_3 are located at 0, 600, 800 and 850, respectively. Obviously, for times $T \ll 1/|H_{gi}|$, the profile is relatively flat with no distinct features.

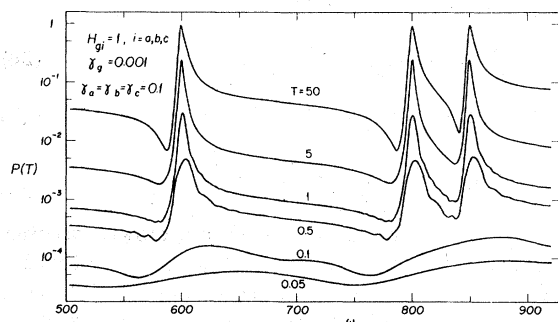


FIG. 2. Ionization probability vs frequency, for the system of Fig. 1 and for a number of pulse lengths T . $H_{gi}^* = H_{gi} = 1$, $\gamma_{gi} = 0.01$, $\gamma_i = \gamma_{ij} = \gamma_j = 0.1$, $i, j = 1-3$, $H_{ij}^* = 0$, and $\gamma_g = 0.001$. The levels g , $a = a_1$, $b = a_2$, and $c = a_3$ are located at the positions $\omega = 0, 600, 800$, and 850 , respectively.

For times $1/|H_{gi}| \ll T \ll 1/\gamma_i$, the maxima have clearly developed, but the minima have not yet really formed. It is clear that for times $T \ll 1/\gamma_i$, the minima are shallow and broad: and for times $T \gg 1/\gamma_i$, they are narrow and deep. In addition, the position of the lowest minimum moves from $\delta \approx -40$ (for $T < 1/|H_{gi}|$), to $\delta \approx -10$ (δ measured from a_1) over a time period of the order of $1/\gamma_i$. The minimum observed for $T \gg 1/\gamma_i$ is at the position which would be predicted by second-order perturbation theory.

In the region $\omega < 650$, these results are quite similar to those which would have been obtained from the simpler BA model by treating a_1 as the only excited bound state and absorbing the effects of a_2 and a_3 into γ_g (as noted above, γ_g can be given an ω dependence). Similarly, other regions of the profile could be reproduced by the BA model by taking a_2 or a_3 as the excited bound state.

We will return to a discussion of these results in Sec. V, where we will use a simple physical picture to explain why the BA model and the many-level model give such similar results for the time evolution of the ionization profile. We shall also present a simple approximation formula for $P(t)$ which describes the ionization profile of the many-level atom well at all times $T \gg 1/|H_{gi}|$.

III. SPONTANEOUS EMISSION

The effect of spontaneous emission on ionization rates is generally simply to broaden out any sharp features such as occur when an intermediate resonance occurs. However, it is certainly possible that spontaneous emission might affect the *development* of resonance profiles in a more complicated fashion. In this section, we introduce a model which enables us to investigate the influence of spontaneous emission on this development.

Spontaneous emission from an atom interacting with a laser beam is very difficult to treat using the quantized field approach of BA and the previous section.⁷ It can, however, be handled in a fairly straightforward fashion by studying the evolution of the atomic density matrix if the fields are treated semiclassically.⁸

Crance and Feneuille⁹ (to be referred to as CF) have introduced a two-level model of atomic photoionization which is the semiclassical field analog of the quantized field model of BA. The predictions of the CF model were shown to agree exactly with the predictions of the BA model when rectangular pulses were used.⁹ In this section we use a modification of the CF model to investigate the effects of spontaneous emission on the time dependence of ionization profiles.

Because classical fields appear in the CF model, one can use this model to set up a density matrix

for the atomic states only. Rewriting Eqs. (9) of CF using the notation of this article one finds

$$i\dot{\alpha}_g = \left(E_g - i\frac{\gamma_g}{2}\right)\alpha_g + e^{i\omega t} \left(H'_{ga} - i\frac{\gamma_{ga}}{2}\right)\alpha_a + i\delta(t), \quad (32)$$

$$i\dot{\alpha}_a = \left(E_a - i\frac{\gamma_a}{2}\right)\alpha_a + e^{-i\omega t} \left(H'_{ag} - i\frac{\gamma_{ag}}{2}\right)\alpha_g, \quad (33)$$

where ω is now the angular frequency of the applied classical field.

Density matrix equations can be derived using the definition

$$\rho_{nm} \equiv \alpha_n \alpha_m^*. \quad (34)$$

Spontaneous emission can be introduced into the resulting equations in a straightforward way following the approach of Mollow and Miller.¹⁰ The resulting equations are

$$\begin{aligned} \dot{\rho}_{aa} &= -(\gamma_a + \Gamma)\rho_{aa} - \gamma_{ga}\varphi - 2\mu H'_{ga}, \\ \dot{\rho}_{gg} &= -\gamma_g\rho_{gg} + \Gamma\rho_{aa} - \varphi\gamma_{ag} + 2\mu H'_{ga} + \delta(t), \\ \dot{\varphi} &= -\varphi(\gamma_a + \gamma_g + \Gamma)/2 + \mu\delta - (\rho_{gg} + \rho_{aa})\gamma_{ga}/2, \\ \dot{\mu} &= -\varphi\delta - \mu(\gamma_a + \gamma_g + \Gamma)/2 - H'_{ga}(\rho_{gg} - \rho_{aa}), \end{aligned} \quad (35)$$

where $|g\rangle$ is the ground state of the atom, $|a\rangle$ the intermediate state, and the off-diagonal density matrix element ρ_{ga} has been written in terms of its real and imaginary parts:

$$e^{-i\omega t} \rho_{ga} = \varphi + i\mu. \quad (36)$$

The quantities γ_a , γ_g , and Γ are as defined above, that is, the inverse lifetime of the excited state $|a\rangle$ due to ionization, the inverse lifetime of the ground state $|g\rangle$ due to ionization through all states other than $|a\rangle$, and the inverse of the spontaneous lifetime of $|a\rangle$ due to decays back to $|g\rangle$, respectively. The detuning is defined in Eq. (1), and

$$H'_{ga} = H_{ga} + \mathcal{P} \int dE \frac{H_{gE} H_{Ea}}{E_g + 2\omega - E}, \quad (37)$$

$$\gamma_{ga} = 2\pi H_{gE} H_{Ea} \Big|_{E=E_g+2\omega}. \quad (38)$$

H_{ga} is the matrix element of $\vec{p} \cdot \vec{A}$ between atomic states $|g\rangle$ and $|a\rangle$, etc.

Equations (35) cannot be solved analytically; they were therefore solved numerically using techniques similar to those used to solve the equations of the previous section. That is, ρ_{aa} , ρ_{gg} , φ , and μ were Fourier transformed, and the resulting algebraic equations were solved for each value of the parameters. An inverse Fourier transform then gave immediately the values of $\rho_{aa}(t)$ and $\rho_{gg}(t)$ (see Appendix).

A number of calculations were made for different values of the parameters appearing in (35). In particular, values of Γ ranging from $10^{-2}\gamma_a$ to $10\gamma_a$ were considered. A typical result is shown in Fig.

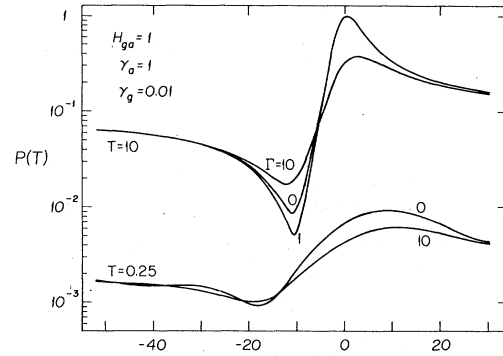


FIG. 3. Probability of ionization of a two-level atom including the effect of spontaneous emission from the excited state. T is the pulse length. $H'_{ga}=1$, $\gamma_a=1$, $\gamma_g=0.01$, $\gamma_{ag}=0.1$. Γ is the inverse spontaneous lifetime of state $|a\rangle$ due to decay to state $|g\rangle$.

3, where $P(T)$ is plotted versus δ for two values of T . This figure was obtained with $\gamma_a=1$, $\gamma_g=0.01$, $\gamma_{ag}=0.1$, and $H'_{ga}=1$. Comparison of the curves with $\Gamma=1$ and 10 to the one calculated for $\Gamma=0$ shows that the main effect of spontaneous emission is to alter the shape somewhat for both maximum and minimum. However, we found that there is no change in the time scale required for the development of either the maximum ($\sim 1/|H_{ga}|$) or the minimum ($\sim 1/\gamma_a$) from the values predicted by BA. In particular, the location of the minimum for $T \ll 1/\gamma_a$ and the location of the minimum for $T \gg 1/\gamma_a$ are almost independent of Γ . Thus, for nonzero Γ there is still a factor of 2 change in the position of the minimum relative to that of the maximum as pulse length increases.

From the numerical calculations, we can obtain an indication of the variation of the shape of the ionization curve with Γ . If $|H_{ga}| \gg \gamma_a$, an increase in Γ causes a relatively small decrease in $P(T)$ at the maximum, and a large decrease (on a logarithmic scale) in $P(T)$ at the minimum. If $\gamma_a \gg |H_{ga}|$, $P(T)$ at the maximum decreases considerably, and $P(T)$ at the minimum increases with an increase in Γ .

We shall return to a consideration of the effects of spontaneous emission in the discussion of Sec. V, where we will consider why Γ plays such a small role in the time evolution of the ionization profile.

IV. PULSE SHAPE

The final variable which we have considered is the pulse shape. Physical considerations, to be discussed in the next section, led us to believe that the important question concerning the pulse

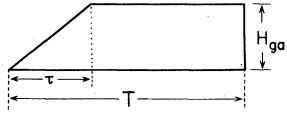


FIG. 4. Radiation pulse shape under consideration.

shape was whether or not the field was turned on adiabatically. Adiabatically, in this case, was felt to most probably mean that the field was turned on slowly compared to the Rabi oscillation of the atom between $|g\rangle$ and $|a\rangle$. Far away from resonance, of course, the Rabi oscillations have a frequency $|\delta|/2\pi$. This situation would correspond to one in which the "Fourier broadening" of the applied field produced by its turn on is less than the detuning from resonance.

In order to investigate the influence of pulse shape on the multiphoton ionization process, we have used the CF model with the pulse shape shown in Fig. 4. The parameter τ , which characterizes the rise time of the pulse, was varied from values $\tau \ll 2\pi/\delta_{\min}$ to values $\tau \gg 2\pi/\delta_{\min}$ where $\delta_{\min} = q\gamma_a/2$ is the value at which the minimum occurs according to second-order perturbation theory.

General aspects of the resonance profile produced by differing pulse shapes have previously been studied using the CF model.⁹ In the present work, we are interested in a very specific aspect of the profile—its evolution in time. As in the previous sections, we shall concentrate on the motion and magnitude of the interference minimum.

One aspect of the results of this calculation is indicated in Fig. 5(a), where we plot the position

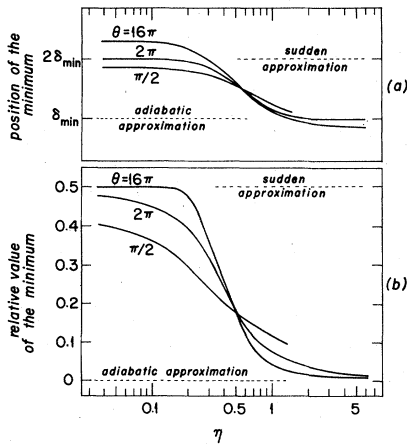


FIG. 5. (a) Position of the ionization profile minimum vs $\eta = \tau\delta_{\min}/2\pi$, $\delta_{\min} = q\gamma_a/2$; q is given by Eq. (5). $H_{ga} = 10^3$, $\gamma_a = 1$, $\gamma_g = 0.1$. θ if the radiation pulse area. (b) Relative value of this minimum (in units of γ_g) vs η .

of the minimum versus $\eta = \tau\delta_{\min}/2\pi$ for $H_{ga} = 10^3$, $\gamma_a = 1$, $\gamma_g = 10^{-1}$. The parameter θ is the pulse area of the radiation. In all cases, the pulse length T was much less than $1/\gamma_a$, i.e., less than the time required for the displacement of the minimum when rectangular pulses are used.

For $\eta \ll 1$, the minimum is at $2\delta_{\min}$; for $\eta \gg 1$ at δ_{\min} . The position of the minimum changes fairly abruptly at $\eta \approx 0.6$. That is to say, if $\eta \gg 1$, the minimum does not move in time, but rather will always be at the position δ_{\min} predicted by perturbation theory. Note that $\eta = 1$ corresponds to a rise time of the pulse $\tau = 2\pi/\delta_{\min}$. Thus $\eta \gg 1$ corresponds to the pulse being turned on adiabatically with respect to the Rabi oscillations.

In Fig. 5(b), we show the relative value of the ionization probability at the minimum as a function of η . Again, the results are essentially the same: for $\eta \ll 1$, the minimum is very shallow, but at $\eta \approx 0.5$, the minimum undergoes a sharp decrease in magnitude. This indicates once more that the minimum produced for $\eta \gg 1$ is essentially that which is predicted by second-order perturbation theory.

One sees then, that the manner in which the field is turned on can have a determining effect in the time evolution of the multiphoton profile, with the key criterion being whether or not the field is turned on adiabatically. We will discuss why this should be so in the next section.

V. DISCUSSION

A. Beers-Armstrong model

Since the results obtained above using the improved models of multiphoton ionization have been compared to results of the BA model, a thorough understanding of the BA model will facilitate discussion of the results of the improved models.

If one uses perturbation theory to obtain approximate solutions of the density matrix equations for the two-photon ionization of a two-level atom, one finds that there are two paths which can be followed in going from ρ_{gg} , the ground-state density, to ρ_{EE} , the density of a continuum state. These two paths are indicated in Fig. 6. The interactions

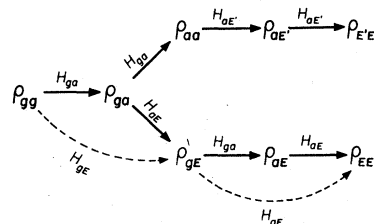


FIG. 6. Paths through which ionization proceeds.

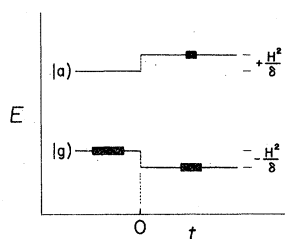


FIG. 7. ac Stark level shifting due to sudden turn-on of the field at $t=0$. $H = H_{ga}$. The heavy lines indicate population (schematic).

written above the arrows in Fig. 7 are those which appear in the perturbation expression linking the various elements of the density matrix. The upper path is often referred to as a "two-step" process since it involves moving population density from $|g\rangle$ into $|a\rangle$ and then on into $|E^*\rangle$, i.e., it contains the sequence $\rho_{gg} \rightarrow \rho_{aa} \rightarrow \rho_{E^*E^*}$. The lower path is referred to as a "two-photon" process, since it does not involve putting the atom into state $|a\rangle$, but rather describes a roughly simultaneous absorption of two photons which takes the atom from $|g\rangle$ to $|E\rangle$. If one considers the dependence of ρ_{EE} on E , one finds additional differences between the two-step and two-photon processes.¹¹ If the field is detuned from the $|g\rangle \rightarrow |a\rangle$ resonance, then the former has a maximum which conserves energy in the last step $|a\rangle \rightarrow |E^*\rangle$. If the power broadening of the intermediate state $|a\rangle$ and its lifetime due to ionization are taken into account, the latter process has its main maximum such that energy is conserved in the overall transition $|g\rangle \rightarrow |E\rangle$. Thus if we consider only the main contributions from the two-step and two-photon processes, we find that $E \neq E^*$ when energy is not conserved in the first step $|g\rangle \rightarrow |a\rangle$. Of course, in a complete, rather than a perturbation, solution of the density matrix equations for two-photon ionization, these paths are not so clearly separable. However, we shall find it convenient to retain this nomenclature when discussing the results which are given in the previous sections.

Let us first consider the BA model, and the reasons why there is a shift in the shape and location of minima of the resonance profile predicted by that model. An understanding of this will make our subsequent discussions much more straightforward. In the BA model, there are additional paths between ρ_{gg} and ρ_{EE} , shown in Fig. 6, which involves the matrix element H_{gE} . Transitions produced by H_{gE} must be energy conserving in the process $|g\rangle \rightarrow |E\rangle$ since H_{gE} is obtained from perturbation theory. There is therefore possibly an interference introduced into the two-photon process by the presence of H_{gE} , e.g., between the indirect path $\rho_{gg} \rightarrow \rho_{aE} \rightarrow \rho_{EE}$ and the direct path $\rho_{gg} \rightarrow \rho_{EE}$, both of which have the same beginning and ending points. This is indicated schematically in Fig. 6. That is

to say, an expression for ρ_{EE} obtained using perturbation theory will reflect the interference between the contributions of the two processes.

Namely, there will be a contribution to ρ_{EE} from the indirect path of the form $\alpha H_{aE} \rho_{aE}$, and a contribution from the direct path of the form $\beta H_{gE} \rho_{gE}$. Depending on the parameters involved, these two terms may make contributions to ρ_{EE} either of the same or of opposite signs. However, the presence of a direct path produced by H_{gE} should not significantly affect the upper two-step path since the maxima of the contributions from these two paths do not coincide in energy. We shall show below that the mathematical predictions of the BA model are explained very well by this interpretation.

Expanding Eqs. (13) and (14) of BA in a power series in $1/\delta$ and keeping only the lowest-order nonvanishing terms involving either H_{ga}/δ or γ_a/δ we find an approximate form of $P(t)$ which is valid for large $|\delta| \gg |H_{ga}|, \gamma_a$ and times $t > 1/|\delta|$:

$$P(t) \cong 1 - (|H_{ga}|^2/\delta^2) \exp(-\gamma_a t) - (1 - |H_{ga}|^2/\delta^2) e^{-\sigma t}, \quad (39)$$

where

$$\sigma = \gamma_g \left(1 + \frac{\gamma_a}{2\delta} \right)^2 = 2\pi \left| H_{gE} + \frac{H_{ga} H_{aE}}{\delta} \right|^2 = 2\pi \left| \sum_i \frac{H_{gi} H_{iE}}{\delta_i} \right|^2 \quad (40)$$

and $\delta_i = E_g + \omega - E_i$. The second term on the right-hand side of Eq. (39), $(|H_{ga}|^2/\delta^2) \exp(-\gamma_a t)$, is approximately equal to $\rho_{aa}(t)$, as can be shown, in a rather tedious way, using the BA model to calculate $|U_{ag}(t)|^2 = \rho_{aa}(t)$, and then making an expansion valid for the conditions given above. This term thus corresponds to the contribution to the total ionization probability from the two-step process. There are obviously no interference effects present in this term. However, the third term on the right-hand side of Eq. (39) clearly does show interference effects (in σ) produced by the presence of H_{gE} ; it is this final term which approximately describes the contribution of the two-photon process to the total ionization probability. The final form given above for σ follows if second-order perturbation theory is used to evaluate H_{gE} . It is obvious from this expression that σ is just the ionization rate which is obtained from lowest nonvanishing order perturbation theory.

In obtaining Eq. (39), we have dropped rapidly oscillating terms of the type $\sin \delta t$ and $\cos \delta t$. These terms are very important for t close to zero, since the $\cos \delta t$ term assures that $\rho_{aa}(0) = 0$, and the $\sin \delta t$ term dominates the rise of $\rho_{aa}(t)$ from zero to the value $|H_{ga}|^2/\delta^2$. However, the combination of these terms tends to average to zero for times $t > |\delta|$.

For pulse lengths $T < 1/\gamma_a$, both exponentials in (39) can be expanded to give

$$P(T) \cong [|H_{ga}|^2 / \delta^2 \gamma_a + \sigma] T. \quad (41)$$

The quantity in brackets above is just the transition rate σ_i of BA taken at large δ . When $T \gg 1/\gamma_a$, but $\ll 1/\sigma$, $\exp(-\gamma_a T) \cong 0$, and

$$P(T) \cong \sigma T \quad (42)$$

σ is, of course, just σ_2 of BA taken at large δ . The ionization profile for $T < 1/\gamma_a$ is therefore seen to be produced by a term with a sharp minimum (σ) superimposed on a term which is smoothly varying in δ ; for $T \gg 1/\gamma_a$, the smoothly varying term disappears.

As indicated above, the value of $\rho_{aa}(t)$ builds up very rapidly after $t=0$ (in a time $1/|\delta|$), and then effectively decays away with a lifetime $1/\gamma_a$. We can interpret this rapid buildup as having been produced by the sudden turn-on of the field. The magnitude of the increase in ρ_{aa} , $|H_{ga}|^2 / \delta^2$, is just that which is necessary to conserve the total energy of the atomic system when the levels are suddenly ac Stark shifted by the applied field (Fig. 7). The excited state $|a\rangle$ then decays via ionization without having its population further replenished since the field is tuned far from resonance. Thus, for large $|\delta|$, except for the population promoted to $|a\rangle$ by the turn on of the field at $t=0$, the atom must decay predominantly via a two-photon process which displays sharp interference effects.

B. Many-level model

By making a perturbation expansion valid away from all resonances of the Green's functions for the two-photon ionization of a many-level atom, one easily finds the approximate ionization probability

$$P(t) \cong 1 - 2\pi \sum_i \left| \frac{H_{gi} H_{iE}}{\delta_i} \right|^2 \exp(-\gamma_i t) - \left(1 - 2\pi \sum_i \left| \frac{H_{gi} H_{iE}}{\delta_i} \right|^2 \right) e^{-\sigma t}, \quad (43)$$

where

$$\sigma = 2\pi \left| \sum_i \frac{H_{gi} H_{iE}}{\delta_i} \right|^2. \quad (44)$$

In Eq. (43), $1/\gamma_i$ is the ionization lifetime of the i th state. Comparison of (43) with (39) shows that the profile predicted for the many-level atom will show a time evolution which is qualitatively the same as that of the two-level BA atom. In particular, one can expect to see interference minima which move and change their shape in time.

Whether or not the predictions of (43) for a particular minimum are quantitatively similar to

those of Eq. (39) depends on whether or not in the region of that minimum one term dominates the sum

$$\sum_i \left| \frac{H_{gi} H_{iE}}{\delta_i} \right|^2 \exp(-\gamma_i t)$$

for all t such that this sum is of the order of σ . This condition is obviously necessary since σ in (43) is identical to σ in (39); that is, the usual second-order perturbation cross section. In general, one can expect one term to be dominant in (43) if the region of the minimum is much closer to one level than to any of the others. This "generally" will not, of course, be true if the matrix elements into or out of this state are unusually small.

C. Spontaneous emission

Equations (35) can also be solved approximately for large δ ; the resulting probability of ionization is quite similar to that given in Eq. (39). Of course, the coefficients $|H_{ga}|^2 / \delta^2$ must be replaced, but the new coefficients show only a weak dependence on Γ and are given to a fair approximation by $|H_{ga}|^2 / (\delta^2 + \frac{1}{4}\Gamma^2)$. This approximate form is exact as $\Gamma \rightarrow 0$, and is off only about a factor of 2 in the region of δ_{\min} when $\Gamma = 10\gamma_a$. The value of σ also changes, but again, the changes are small. The main difference between the solutions to Eqs. (35) and (39) is that $\exp(-\gamma_a t)$ is replaced by $\exp[-(\gamma_a + \Gamma)t]$.

Following the arguments of Sec. V A, one might then expect that the changes in the shape and position of the minimum would in this case occur with a characteristic time $1/(\gamma_a + \Gamma)$. This, however, is not correct, as can easily be shown if we consider Eq. (39) with γ_a replaced by $\gamma_a + \Gamma$:

$$P(t) \cong 1 - \left[\frac{|H_{ga}|^2}{\delta^2} \exp[-(\gamma_a + \Gamma)t] + \left(1 - \frac{|H_{ga}|^2}{\delta^2} \right) e^{-\sigma t} \right]. \quad (45)$$

This equation should provide a fairly good approximation if $\delta \gg \Gamma$, $|H_{ga}|, \gamma_a$. Once again, we are interested in the variation of $P(t)$ in the region of δ_{\min} . Let us consider an extreme case where $\exp[-(\gamma_a + \Gamma)t]$ rapidly decays away, leaving the expression

$$P(t) \cong 1 - (1 - |H_{ga}|^2 / \delta^2) e^{-\sigma t}, \quad t > 1/(\gamma_a + \Gamma). \quad (46)$$

Expanding the exponential, one obtains

$$P(t) \cong |H_{ga}|^2 / \delta^2 + \sigma t + \dots \quad (47)$$

In the region around δ_{\min} , the first term in this series has the magnitude γ_g / γ_a . The second term is approximately equal to $\gamma_g t$ except very near to δ_{\min} , where it has a sharp minimum. Thus the smoothly varying (in δ) first term in $P(t)$ will dom-

inate the probability in the region around δ_{\min} until $t \gg 1/\gamma_a$. The situation is thus qualitatively as in the BA model, and one observes a minimum which moves and changes its shape on a time scale $1/\gamma_a$.

D. Pulse shape

If the reasoning of Sec. VA is correct, the moving minimum observed in the BA model is, in effect, produced by the nonadiabatic turn on of the driving field. If the field is turned on adiabatically, there will be no populating of $|a\rangle$ at $t=0$ due to the turn on of the field. Furthermore, for large detuning, there will be no population promoted to $|a\rangle$ by the field for $t>0$. Thus there will be no superposition of cross sections such as occurred in Eq. (39) which leads to the short-time behavior of BA.

The calculations discussed in Sec. IV fully support this interpretation of the BA results. That is, the transition rate abruptly changes to the second-order perturbation rate when the rise time of the pulse is approximately equal to $1/\delta_{\min}$, the criterion for an adiabatic turn on of the field.

VI. CONCLUSIONS

We have made a number of improvements to the BA model, and have considered the effects of these improvements on the predicted short-time behavior of two-photon ionization. In particular, we have considered the effects produced by treating more levels of the atom explicitly, by introducing spontaneous emission, and by the shape of the pulse. The first two of these changes in the model cause no qualitative changes in the predictions of BA; the last of these effects was shown to be of critical importance. We have discussed the reasons why these improvements in the model either did or did not significantly effect the predictions, and showed that the results can be interpreted as a competition between two-step and two-photon modes of ionization. We note that this discussion indicated that for short time periods, the two-step process could be quite important even when the first step was considerably detuned from resonance. This is in contrast to a conclusion of Chebotayev¹¹ reached by an analysis based on time-independent perturbation theory alone.

These calculations imply that either the type of minimum in the cross section predicted by Feneuille and Armstrong³ or the phenomena of a moving minimum¹ should be observable in principle. However, in practice, both of these will be extremely difficult to observe due to the requirement that the field be turned on fast with respect to the inverse of the detuning from resonance at the minimum.

ACKNOWLEDGMENT

This work was supported in part by the NSF.

APPENDIX

We outline here the numerical procedure for efficiently calculating $\alpha_m(t)$, $m=g, \{i\}$ in Eq. (18) via their Fourier transforms $G_m(z)$.

Equation (25) can be written as a matrix equation:

$$\tilde{A}\underline{G} = (\underline{A}-z\underline{1})\underline{G} = \underline{B}, \quad (\text{A1})$$

where

$$\underline{A} = \begin{bmatrix} W_g^* - i\gamma_g/2 & H_{ga}^* - i\gamma_{ga}/2 & \cdots \\ H_{ga}^* - i\gamma_{ga}/2 & W_a^* - i\gamma_a/2 & \cdots \\ \vdots & \vdots & \ddots \end{bmatrix}; \quad (\text{A2})$$

$$\underline{1} = \begin{bmatrix} 1 & 0 \\ & 1 \\ 0 & 1 \end{bmatrix}; \quad \underline{B} = \begin{bmatrix} -1 \\ 0 \\ 0 \\ \vdots \end{bmatrix}; \quad \underline{G} = \begin{bmatrix} G_g \\ G_a \\ \vdots \end{bmatrix}.$$

The solution of (A1) will be formally given by

$$G_m = \frac{\det \tilde{A} | \tilde{A}_{n, m=B_n}}{\det \tilde{A}}. \quad (\text{A3})$$

The determinant in the denominator can be expressed as a function of the eigenvalues of matrix \underline{A} :

$$\det \tilde{A} = \det [\underline{A} - z\underline{1}] = \prod_{i=1}^n (\lambda_i - z). \quad (\text{A4})$$

Consequently the Fourier transform Eq. (21) of G_m will be

$$\alpha_m(t) = -\frac{1}{2\pi i} \int_{-\infty}^{+\infty} dz e^{-izt} \left(C_m(z) / \prod_{i=1}^n (\lambda_i - z) \right), \quad (\text{A5})$$

where $C_m(z)$ is the determinant of the matrix obtained from \underline{A} by replacing its m column with matrix \underline{B} .

The evaluation of (A5) is immensely facilitated by the use of the theory of residues; namely, since we are considering only $t>0$ the integral in (A5) is equal to the contour integral along the path shown in Fig. 8. The latter integral is then equal to $-2\pi i \times$ (the sum of residues of the integrand function). This sum includes only the eigenvalues λ_i with $\text{Im} \lambda_i < 0$; it turns out that all the eigenvalues of \underline{A} possess this property.

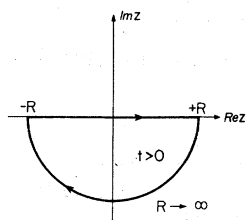


FIG. 8. Integration contour for Eq. (A5).

Thus

$$\alpha_m(t) = \sum_{k=1}^{\eta} \left(C_m(\lambda_k) \exp(-i\lambda_k t) / (-1) \prod_{i=1, i \neq k}^{\eta} (\lambda_i - \lambda_k) \right). \quad (\text{A6})$$

We note here the distinct advantages of this method of evaluating $\alpha_m(t)$ versus the widely used direct integration of Eqs. (31): (a) In dealing with a realistic problem one may have to treat *large* detunings of the order of 0–1 eV, $1 \text{ eV} \approx 10^{15} \text{ sec}^{-1}$ ($\hbar = 1$). The experimentally typical pulse durations

are 1 psec–100 nsec. In solving Eq. (31) with $\delta \sim 1$ eV one then deals with oscillating factors with phase $\delta t = 10^3$ – 10^7 . In order to follow such oscillations one should need 10^4 – 10^9 integration steps for each value of δ . This would require prohibitively large time even for a medium size computer. (b) With such a number of steps the possibility of overwhelming roundoff errors is introduced to the degree of doubting the significance of the results. (c) The necessary computation time is proportional to the pulse duration in the direct integration case, whereas independent of it in the present approach. (d) One can see more transparently the various contributions to the ionization probability, especially through the roots λ_k whose imaginary parts are the “effective” ionization lifetimes of the respective levels.

The present procedure is similarly applied to Eqs. (36) by solving the algebraic system of equations of the Fourier transforms for ρ_{gg} , ρ_{aa} , φ , and μ .

*Present address: Fakultät für Physik der Universität Freiburg, Hermann-Herder-Strasse 3, D-7800 Freiburg/I. Br., West Germany.

†Present address: Joint Institute for Laboratory Astrophysics, Univ. of Colorado, Boulder, Colo. 80309.

¹B. L. Beers and L. Armstrong, Jr., *Phys. Rev. A* **12**, 2447 (1975); L. Armstrong, Jr. and B. L. Beers, in *The Physics of Electronic and Atomic Collisions*, Proceedings of the X ICPEAC, Paris, 1977, edited by G. Watel (North-Holland, Amsterdam, 1978).

²L. Armstrong, Jr., B. L. Beers, and S. Feneuille, *Phys. Rev. A* **12**, 1903 (1975).

³S. Feneuille and L. Armstrong, Jr., *J. Phys. (Paris)* **36**, L235 (1975).

⁴L. Mower, *Phys. Rev.* **142**, 799 (1966).

⁵W. Heitler, *The Quantum Theory of Radiation* (Clarendon, Oxford, 1960).

⁶S. N. Dixit and P. Lambropoulos, Abstracts of the ICOMP, Rochester, N. Y., 1977, p. 202 (unpublished).

⁷C. Cohen-Tannoudji and S. Reynaud, in *Multiphoton Processes*, edited by J. H. Eberly and P. Lambropoulos (Wiley, New York, 1978), p. 103.

⁸B. R. Mollow, *Phys. Rev. A* **12**, 1919 (1975).

⁹M. Crance and S. Feneuille, *Phys. Rev. A* **16**, 1587 (1977).

¹⁰B. R. Mollow and H. M. Miller, *Ann. Phys. (N.Y.)* **52**, 464 (1969).

¹¹V. P. Chebotayev, in *High Resolution Laser Spectroscopy*, edited by K. Shimoda (Springer-Verlag, Berlin, 1976), Eq. (6.22) and the discussion following it. The author discusses transitions between three bound states. However, the solutions to the equations involving two bound states (no spontaneous decay) and the continuum are identical in the approximation used by Chebotayev if one takes $\gamma_1 = \gamma_2 = 0$; γ_0 is the decay rate of the intermediate state due to ionization. Effects of power broadening of a $|a\rangle$ due to H_{ag} can also be included in γ_0 in a perturbative fashion.